Quantum interference effects and spin-orbit interaction in quasi-one-dimensional wires and rings

Ç. Kurdak
Department of Electrical Engineering, Princeton University, Princeton, New Jersey 08544

A. M. Chang, A. Chin, and T. Y. Chang
AT&T Bell Laboratories, Holmdel, New Jersey 07733
(Received 24 February 1992)

We study two kinds of quantum interference effects in transport—the Aharonov-Bohm effect and the weak-localization effect—in quasi-one-dimensional wires and rings to address issues concerning the phase-coherence length, spin-orbit scattering, and the flux cancellation mechanism which is predicted to be present when the elastic mean free path exceeds the sample width. Our devices are fabricated on $GaAs/Al_xGa_{1-x}As$ and pseudomorphic $Ga_xIn_{1-x}As/Al_xIn_{1-x}As$ heterostructure materials and the experiments carried out at 0.4–20 K temperatures. In the $GaAs/Al_xGa_{1-x}As$ devices which exhibit no significant spin-orbit scattering, we were able to extract a phase-coherence length l_ϕ from the amplitude of the Aharonov-Bohm magnetoresistance oscillations in different sized rings. We find it to be in agreement with l_ϕ deduced from the weak-localization data in parallel wires when the one-dimensional weak-localization theory *including the flux cancellation mechanism* is used to fit the data. We therefore unambiguously establish that the same l_ϕ governs the behavior of the two quantum interference phenomena of Aharonov-Bohm oscillations and weak localization, and that the flux cancellation is in force. In the pseudomorphic $Ga_xIn_{1-x}As/Al_xIn_{1-x}As$ heterostructure devices which exhibit strong spin-orbit interaction effects, l_ϕ exceeds the spin-orbit-scattering length at low temperatures. The amplitude of Aharonov-Bohm oscillations can only be explained by introducing reduction factors due to spin-orbit scattering.

I. INTRODUCTION

There has been increasing interest in the study of very small conductors which exhibit a large variety of new physics at very low temperatures. These effects are mainly due to quantum-mechanical interference of electron wave functions; therefore they are known as quantum interference effects. These include the familiar weak-localization (WL) effect which is manifested in the negative magnetoresistance peak around zero magnetic field, the Aharonov-Bohm (AB) effect in doubly connected geometries, and the universal conductance fluctuations (UCF) in mesoscopic devices. The length scale relevant for observing these effects is the phase coherence length $l_\phi=\sqrt{D\tau_\phi}$, where D is the diffusion constant and τ_ϕ is the time between phase breaking collisions. Quantum interference effects are reduced in size at high temperatures due to the decrease in l_ϕ. In most experiments l_ϕ is obtained from weak-localization magnetoresistance and, more recently, from universal conductance fluctuations.[1] In principle, since all these effects arise from quantum interference, they should be governed by the same l_ϕ. To date, however, this hypothesis has yet to be experimentally established. It is the aim of this work to establish the consistency of l_ϕ independently deduced from the AB and WL effects. To this end, we extract the phase-coherence length l_ϕ independently from AB magnetoresistance oscillations and from weak localization and show that the values deduced are in close agreement. In addition, we study the influence of spin-orbit scattering on these effects. We find a reduction in the amplitude of AB oscillations in rings and positive magnetoresistance in wires.

The system we study is the quasi-one-dimensional III-V semiconductor heterostructure wires and rings. We chose semiconductors instead of metal wires because of the long elastic-scattering length l_e which readily exceeds the width W of the wire. This allows us to address the issue of the presence of the flux cancellation mechanism due to multiple reflection off specular sidewalls not present in diffusive wires.[2,3] To address the issue of spin-orbit scattering, we compare effects in $GaAs/Al_xGa_{1-x}As$ and pseudomorphic $Ga_xIn_{1-x}As/Al_xIn_{1-x}As$ heterostructure devises. The $GaAs/Ga_xAl_{1-x}As$ heterostructure devices typically have lower carrier densities and do not exhibit significant spin-orbit scattering effects. In contrast, the pseudomorphic $Ga_xIn_{1-x}As/Al_xIn_{1-x}As$ heterostructure devices show strong spin-orbit interaction as a result of the significantly higher carrier density exceeding 10^{12} cm^{-2},[2,4,5] and positive magnetoresistance is clearly visible in two- or one-dimensional samples. This material also exhibits a long l_ϕ; we have observed AB magnetoresistance oscillations up to 20 K in temperature in a ring of 5.2 μm perimeter.

Effects in quasi-one-dimensional wires can be quite different from those in two- or one-dimensional diffusive wires.[6–10] In this regime, the boundary scatterings become extremely important and the one-dimensional weak-localization theory for diffusive wires given by Al'tshuler and Aronov[11] (AA) for which $l_e \ll w$ would not be applicable. For the case $l_e \gg w$, Dugaev and

Khmel'nitskii investigated the weak-localization conductance of a thin metal film in a magnetic field parallel to the boundary.[2] Their idea of flux cancellation was then extended by Beenakker and van Houten (BvH) to explain weak-localization experiments in ballistic wires, such as ours.[3] So far, nearly all low-field magnetoresistance measurements in ballistic wires have been fitted equally well by the AA and BvH theories,[6–8] mainly because there are too many unknown parameters involved in the characterization of these wires. Recent work by Greene *et al.* agreed only with the AA theory, putting the importance of the flux cancellation mechanism in doubt.[9] The discrepancy observed between their experiment and the BvH theory is explained by small-angle scattering. In our work the weak-localization data obtained from the $GaAs/Al_xGa_{1-x}As$ narrow wires also fitted well with both the AA and BvH theories. However, the phase-coherence length l_ϕ deduced from the BvH theory is in close agreement with that deduced from the AB effect, while the values deduced from the AA theory is about a factor of 2 lower.

The influence of spin-orbit scattering on weak localization is well known and leads to the familiar positive magnetoresistance peak superimposed on the negative magnetoresistance background.[12–14] We observed this behavior in our narrow wires fabricated on the pseudomorphic $Ga_xIn_{1-x}As/Al_xIn_{1-x}As$ heterostructure, and the data are only fitted reasonably with the modified one-dimensional BvH theory which includes the flux cancellation mechanism and spin-orbit interaction. Recent attention has focused on reduction in the amplitude of UCF fluctuations [5] and the AB oscillations.[15] In our experiment on pseudomorphic $Ga_xIn_{1-x}As/Al_xIn_{1-x}As$ rings, we also observe a reduction in the AB oscillation amplitude compared to that expected in the absence of spin-orbit scattering. However, we are in a regime where l_ϕ and l_{SO} are comparable and therefore cannot compare our results directly with the existing theories on strong or weak spin-orbit scattering. Nevertheless, the best fit is achieved by introducing a spin-orbit relaxation factor into the scaling equation for the amplitude of AB oscillations.

II. THEORETICAL BACKGROUND

A. Weak localization

Quantum-mechanical corrections to the Boltzmann conductivity in dirty metals are present at low temperatures due to the coherent interference of electrons from time-reversal paths. These corrections have been studied under the name of weak localization. Application of a magnetic field destroys the time-reversal symmetry and, therefore, the coherent interference of electrons. From the experimental point of view, the magnetic field is a very powerful tool to study weak localization. The observed negative magnetoresistance behavior in dirty metals has been fitted extremely well with the weak-localization theories.

The weak-localization correction to the conductance of a wire in the presence of a magnetic field can be written as

$$\Delta G(B)=-\frac{2e^2}{\pi\hbar}\frac{D}{L}\int_0^\infty dt\, C(t)e^{-t/\tau_\phi}e^{-t/\tau_B}, \tag{1}$$

where D is the diffusion constant and L is the length of the sample.[16] The function $C(t)$ is the probability density for an electron to return to the origin. The exponentials in the integrand are the phase and magnetic relaxation factors. $C(t)=\sqrt{4\pi Dt}$ is known from the solution of the one-dimensional diffusion equation. Thus, by taking the integral in Eq. (1) we obtain

$$\Delta G(B)=-\frac{e^2}{\pi\hbar}\frac{\sqrt{D}}{L}\left[\frac{1}{\tau_\phi}+\frac{1}{\tau_B}\right]^{-1/2}. \tag{2}$$

Al'tshuler and Aronov have shown[11] that for a diffusive ($l_e \ll w$) wire in a perpendicular magnetic field, τ_B can be written as

$$\tau_B=\frac{6l_B^4}{w^2v_f^2\tau_e}, \tag{3}$$

where w is the width of the wire and $l_B=\sqrt{\hbar/eB}$ is the magnetic length. In ballistic ($l_e \gg w$) wires Eq. (3) is not valid any more, mainly because the specular boundary scatterings become extremely important. Dugaev and Khmel'nitskii showed that, when the magnetic field is parallel to the surface of a thin metal film, a closed path of an electron scattering only from the surface of the walls encloses zero flux, an effect known as flux cancellation.[2] Such paths thus do not contribute to the magnetoresistance. Later, using flux cancellation, Beenakker and van Houten modified Eq. (3) to extend weak-localization theory to ballistic wires,[3] as

$$\tau_B=\frac{l_B^4}{K_1w^3v_f}+\frac{l_B^2\tau_e}{K_2w^2}. \tag{4}$$

The coefficients K_1 and K_2 depend on the nature of boundary scatterings: $K_1=0.11$ and $K_2=0.23$ for specular scatterings, and $K_1=\frac{1}{4}\pi$ and $K_1=\frac{1}{3}$ for diffusive scatterings. As far as magnetoresistance data are concerned, the contribution of flux cancellation is equivalent to a reduction in effective area of the wire. Furthermore, they pointed out that $C(t)$ used in the AA theory is only valid in the long-time regime, therefore they used $C(t)=(4\pi Dt)^{-1/2}(1-e^{-t/\tau_e})$ in order to take into account short-time corrections. Thus, they modified Eq. (2) as

$$\Delta G(B)=-\frac{e^2}{\pi\hbar}\frac{\sqrt{D}}{L}\left[\left[\frac{1}{\tau_\phi}+\frac{1}{\tau_B}\right]^{-1/2}-\left[\frac{1}{\tau_\phi}+\frac{1}{\tau_e}+\frac{1}{\tau_B}\right]^{-1/2}\right]. \tag{5}$$

Note that $\Delta G(B)$ is reduced with the addition of this new term. In the limit when $\tau_\phi \gg \tau_e$ Eqs. (2) and (5) are essentially identical.

B. Aharonov-Bohm effect

At very low temperatures, the resistance of small doubly connected rings exhibit periodic oscillations in a mag-

netic field; this is known as the Aharonov-Bohm effect. The oscillations come from the interference of propagating electron waves which split up into two partial waves and recombine after acquiring different phases. The phase difference arises from the different path lengths and the magnetic flux encircled by the path of the electron wave function. The magnetic field that causes a phase difference of 2π should be the period of the AB oscillations. For a ring of area A the period is $\Delta B_{\rm AB}=h/eA$.

There are two important characteristic lengths, namely, thermal length $L_T=\sqrt{D\hbar/kT}$ and phase-coherence length l_ϕ, which contribute to the size of the Aharonov-Bohm oscillations. When both of these length scales are much longer than the perimeter of the ring (as temperature goes to zero), the root mean square (rms) of the AB oscillations in conductance $\Delta g_{\rm AB}$ is expected to be on the order of the universal value e^2/h, which was originally predicted for universal conductance fluctuations.[17] The scaling of the amplitude of the AB oscillations with these characteristic lengths is experimentally studied by looking at the temperature dependence of these oscillations. In small noble-metal rings the amplitude of the AB oscillations in magnetoresistance showed a temperature dependence of $T^{-1/2}$, which is explained by the energy averaging of conduction channels.[18] Later, Milliken *et al.* performed experiments on Sb rings, and they observed an exponential drop in the amplitude of the AB oscillations $\exp(-L/l_\phi)$ where L is the length of the sample.[19] By combining the energy averaging factor and the exponential drop, the amplitude of the AB oscillations can be written as follows:

$$\Delta g_{\rm AB}=\gamma\frac{e^2}{h}\left[\frac{\pi^2\hbar D}{p^2kT}\right]^{1/2}\exp(-\alpha p/l_\phi)\ , \tag{6}$$

where D is the diffusion coefficient, p is the perimeter of the ring, and γ is a number on the order of unity. This equation is essentially the same as the one given by Milliken *et al.*, but to be more general we preferred to write $\exp(-L/l_\phi)$ as $\exp(-\alpha p/l_\phi)$ where α is the decay exponent which should be a universal number for a given ring geometry.

The prefactor $(\pi^2\hbar D/p^2kT)^{1/2}$ in Eq. (6) is due to energy averaging and is only valid for the asymptotic case in which the thermal length L_T is much smaller than the perimeter of the ring. In the other limit, when L_T is much bigger than the perimeter, the prefactor should be replaced by 1.

DiVincenzo and Kane calculated numerically the scaling of AB oscillations for the geometry of Fig. 1(a).[20] They predict that the nonlocal resistance $R_{1,2;4,3}$ where the four-point resistance $R_{i,j;k,l}$ is defined as the ratio of voltage measured between leads k and l to the current passed through leads i and j, would decay with an exponent of $\alpha=0.63$. On the other hand, they could not describe the decay of the local resistance $R_{1,4;2,3}$ as a single exponent. Their calculation suggests that for most of the experiments in which p/l_ϕ is restricted to a small range of $1.5<p/l_\phi<3$, the effective decay of the local resistance is slightly faster than the nonlocal one. Furthermore, they pointed out that the energy averaging prefactor, introduced by Milliken *et al.*, in Eq. (6) is not quite right and should be replaced by $(\hbar D/p^{0.7}l_\phi^{1.3}kT)^{1/2}$ which would lead to a new scaling expression as

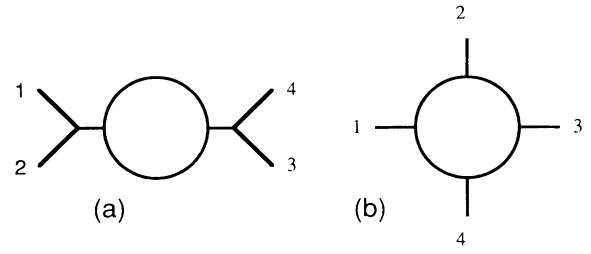

FIG. 1. (a) The doubly connected Aharonov-Bohm ring used in the calculations of DiVincenzo and Kane. (b) The ring pattern used in our experiments.

$$\Delta g_{\rm AB}=\gamma\frac{e^2}{h}\left[\frac{\hbar D}{p^{0.7}l_\phi^{1.3}kT}\right]^{1/2}\exp(-\alpha p/l_\phi)\ . \tag{7}$$

Note that this equation also explains the $T^{-1/2}$ dependence of $\Delta g_{\rm AB}$ observed in metal rings where l_ϕ saturates at very low temperatures. In order to clarify the physics behind these prefactors, we would like to review the energy averaging of conduction channels and a somewhat simplified picture of the AB effect given by DiVincenzo *et al.* Later, we will modify this picture to explain the influence of the spin-orbit interaction on the AB effect.

Electrons which are separated in energy by more than the correlation energy E_c do not contribute to AB conductance with the same phase. At high temperatures, when $kT>E_c$, one has to average out the contribution of electrons within kT of the Fermi energy, which would give an energy averaging factor of $(E_c/kT)^{1/2}$. For an AB ring geometry $E_c=\hbar/t_{\rm int}$ where $t_{\rm int}$ is the interference time. Now, let us define $P(t)$ as the probability density that an electron will interfere with itself after diffusing around the ring after some time interval t. If the perimeter of the ring is bigger than the scattering length, $P(t)$ can be approximately written as

$$P(t)=e^{-p^2/Dt}e^{-t/\tau_\phi}\ , \tag{8}$$

where the first and the second exponents are the probabilities, in a time interval t, that the electron will diffuse around the ring and retain its phase memory. The amplitude of AB oscillations should be proportional to the integral of $P(t)$ over t. For the electrons which contribute to the AB effect the most, the interference time $t_{\rm int}=pl_\phi/D$ is obtained by maximizing $P(t)$. This would give us an energy averaging factor of $(\hbar D/pl_\phi kT)^{1/2}$ which is closer to the numerical calculation of DiVincenzo and Kane.

Since Eqs. (6) and (7) only differ in the prefactor, experimentally it is very difficult to resolve the difference of these theories. Following the above argument which captures the basic physics of the AB effect, we believe that Eq. (7) is a more correct scaling equation for the size of the AB oscillations, although we will use both of these equations for comparison. We would expect for our

four-point resistance $R_{1,4;2,3}$ [Fig. 1(b)] the effective exponent α to be in between the exponents of the local and nonlocal resistances discussed above. In analyzing our data we will take $\alpha=0.63$.

C. Spin-orbit interaction

Hikami, Larkin, and Nagaoka studied the quantum conductance of two-dimensional disordered systems in the presence of spin-orbit scattering.[12] The main prediction of their theory was the change in sign of the weak-localization term, which was later experimentally confirmed by the observation of positive magnetoresistance.[13]

We would like to extend the theory given above for the weak-localization correction to the conductance of a one-dimensional wire to include spin-orbit scattering. This can be done by simply adding a spin-orbit relaxation factor[16] to Eq. (1) as

$$\Delta G(B)=-\frac{2e^2}{\pi\hbar}\frac{D}{L}\int_0^\infty dt\, C(t)e^{-t/\tau_\phi} \times\tfrac{1}{2}(3e^{-4t/3\tau_{SO}}-1)e^{-t/\tau_B} . \quad (9)$$

Here, we assume that the spin-orbit scattering time τ_{SO} is isotropic. Thus by taking the above integral we obtain

$$\Delta G(B)=-\frac{e^2}{\pi\hbar}\frac{\sqrt{D}}{L}\left[\frac{3}{2}\left[\frac{1}{\tau_\phi}+\frac{4}{3\tau_{SO}}+\frac{1}{\tau_B}\right]^{-1/2} -\frac{1}{2}\left[\frac{1}{\tau_\phi}+\frac{1}{\tau_B}\right]^{-1/2} -\frac{3}{2}\left[\frac{1}{\tau_\phi}+\frac{4}{3\tau_{SO}}+\frac{1}{\tau_e}+\frac{1}{\tau_B}\right]^{-1/2} +\frac{1}{2}\left[\frac{1}{\tau_\phi}+\frac{1}{\tau_e}+\frac{1}{\tau_B}\right]^{-1/2}\right] \quad (10)$$

which is very similar to the equation given by Santhanam, Wind, and Prober.[21] In the strong spin-orbit interaction limit the exponential term in the spin-orbit relaxation factor is suppressed, and the reduction factor becomes $-\frac{1}{2}$ which is the same as the two-dimensional result. Also, similar to the two-dimensional case, magnetoresistance starts out positive but changes sign at higher magnetic fields when τ_B becomes smaller than τ_{SO}. In the presence of flux cancellation, when Eq. (4) is used, resistance maxima occur at a higher magnetic field.

Scaling of the amplitude of the AB oscillations has not been studied in the presence of spin-orbit scattering. We will modify the simple picture of the AB effect given above to illustrate the influence of spin-orbit interaction. By adding the same spin-orbit relaxation factor, we can rewrite Eq. (8) as

$$P(t)=e^{-p^2/Dt}e^{-t/\tau_\phi}\tfrac{1}{2}(3e^{-4t/3\tau_{SO}}-1) . \quad (11)$$

The spin-orbit reduction factor can significantly suppress the amplitude of the AB oscillations. It is not even clear to us that a simple scaling expression can be written for the amplitude of the AB oscillations when τ_ϕ and τ_{SO} are comparable. We will only consider strong and weak spin-orbit interaction limits.

For weak spin-orbit interaction the reduction factor is roughly $e^{-2t/\tau_{SO}}$. We can use the same scaling equation by replacing τ_ϕ by $\tau_{\phi\text{eff}}$, where $\tau_{\phi\text{eff}}$ is defined by

$$\frac{1}{\tau_{\phi\text{eff}}}=\frac{1}{\tau_\phi}+\frac{2}{\tau_{SO}} . \quad (12)$$

This equation is valid for other quantum interference effects as well.

On the other hand, in the strong spin-orbit interaction limit, the spin-orbit relaxation factor can be approximated as $\frac{1}{2}(3e^{-4t_{int}/3\tau_{SO}}-1)$ which would lead to a generalized scaling equation of

$$\Delta g_{AB}=\gamma\frac{e^2}{h}\left[\frac{E_c}{kT}\right]^{1/2}\tfrac{1}{2}(3e^{-4\hbar/3E_c\tau_{SO}}-1) \times\exp(-\alpha p/l_\phi) . \quad (13)$$

The correlation energy used by Milliken *et al.*, $E_c=\hbar D/p^2$, does not depend on temperature, so for a given ring the spin-orbit reduction factor can be absorbed in the prefactor γ. However, if we use $E_c=\hbar D/p^{0.7}l_\phi^{1.3}$, the temperature dependence of AB oscillations with or without the spin-orbit reduction factor can be quite different. It is important to realize that in this asymptotic limit, the spin-orbit reduction factor gets smaller with decreasing spin-orbit coupling.

III. EXPERIMENT

A. Material and device characteristics

Quantum interference effects in quasi-one-dimensional wires are studied in five different samples. The starting materials were GaAs/$Al_{0.3}Ga_{0.7}$As and pseudomorphic $Ga_{0.2}In_{0.8}As/Al_{0.48}In_{0.52}As$ modulation-doped heterostructures grown by molecular-beam epitaxy (MBE). The details of the growth process for the pseudomorphic $Ga_xIn_{1-x}As/Al_xIn_{1-x}As$ heterostructure are given elsewhere.[22] We measured the two-dimensional electron gas densities and the Hall mobilities of these materials at 4 K using standard Hall bar geometry. The GaAs/Al_xGa_{1-x}As was uniform with an average two-dimensional electron density n_s and Hall mobility μ of 5.6×10^{11} cm^{-2} and 420 000 cm^2/V sec, respectively. The pseudomorphic $Ga_xIn_{1-x}As/Al_xIn_{1-x}As$ was very nonuniform, especially near the edges of the wafer where the two-dimensional electron densities changed from 1.7×10^{12} to 0.7×10^{12} cm^{-2}; correspondingly the Hall mobilities changed from 160 000 to 70 000 cm^2/V sec.

The materials on which the samples were fabricated, the patterns used in these samples, and the carrier densities n_s obtained from Shubnikov–de Haas (SdH) oscillations are shown in Table I. Two of the samples had an AB pattern which consisted of rings with perimeters of 5.2, 6.7, 7.8, and 8.8 μm, and the other three samples had a WL pattern which consisted of 16 parallel 45-μm wires on them. The width of the wires used in both patterns was 0.45 μm. The patterns were defined by using

TABLE I. Materials on which our samples were fabricated, the patterns used in these samples, and the carrier densities n_s obtained from SdH oscillations.

	Material	Pattern	Carrier density ($1/cm^2$)
Sample 1	$GaAs/Al_xGa_{1-x}As$	AB	0.5×10^{12}
Sample 2	pseudo. $Ga_xIn_{1-x}As/Al_xIn_{1-x}As$	AB	1.5×10^{12}
Sample 3	$GaAs/Al_xGa_{1-x}As$	WL	0.5×10^{12}
Sample 4	pseudo. $Ga_xIn_{1-x}As/Al_xIn_{1-x}As$	WL	0.8×10^{12}
Sample 5	pseudo. $Ga_xIn_{1-x}As/Al_xGa_{1-x}As$	WL	1.5×10^{12}

electron-beam lithography, followed by metalization, photolithography, and wet etching. The details of the fabrication process are described elsewhere.[23]

B. Data presentation

We made four terminal magnetoresistance measurements between 0.4 and 20 K in a He^3 refrigerator where the magnetic field was perpendicular to the sample. The data were taken using a lock-in amplifier at 23 Hz and the current levels kept low enough to avoid self-heating. We studied quantum interference effects only at low magnetic fields ($B < 1$ kG). At high magnetic fields we observed Shubnikov–de Haas oscillations which we used to obtain carrier densities. Typically, the electron densities of the narrow wires were about 10% lower than the two-dimensional electron densities of the starting material.

Weak-localization measurements were made in an array of 16 parallel wires. The length of the wires was chosen to be much longer than the phase-coherence length in order to suppress the contribution of universal conductance fluctuations. Figures 2(a) and 2(b) show the four-point resistance of the narrow wires of the $GaAs/Al_xGa_{1-x}As$ and the pseudomorphic $Ga_xIn_{1-x}As/Al_xIn_{1-x}As$ samples as a function of magnetic field at 0.5 K. Several typical features of low-field magnetoresistance data can be identified in this plot. First, the data is very symmetric under magnetic field reversal. Second, in the pseudomorphic $Ga_xIn_{1-x}As/Al_xIn_{1-x}As$ data there is a small magnetic-field region around zero magnetic field where the magnetoresistance is positive, and at higher magnetic fields the magnetoresistance changes sign. Last, there is a parabolic background resistance which is a slowly varying function of magnetic field.[24] The positive magnetoresistance behavior was only present in the samples fabricated on the pseudomorphic $Ga_xIn_{1-x}As/Al_xIn_{1-x}As$ heterostructure. With increasing temperature the positive magnetoresistance behavior around zero magnetic field disappeared, and later the negative magnetoresistance peak decreased in size. On the other hand, the background resistance was independent of temperature. In the calculation of the weak-localization contribution to conductance $\Delta G(B)$ we subtracted this parabolic background resistance, even though in the magnetic-field range of our analysis the contribution of the parabolic background was not significant.

In Figs. 3 and 4, we show the magnetoresistance data for a 7.8-μm ring of $GaAs/Al_xGa_{1-x}As$ and a 5.2-μm ring of pseudomorphic $Ga_xIn_{1-x}As/Al_xIn_{1-x}As$ samples at different temperatures. The four-point resistance shows periodic AB oscillations in a magnetic field with the expected period of h/eA. In the pseudomorphic $Ga_xIn_{1-x}As/Al_xIn_{1-x}As$ sample AB oscillations are observable at 19 K which is much higher compared to 4 K in $GaAs/Al_xGa_{1-x}As$. This indicates a longer l_ϕ in this

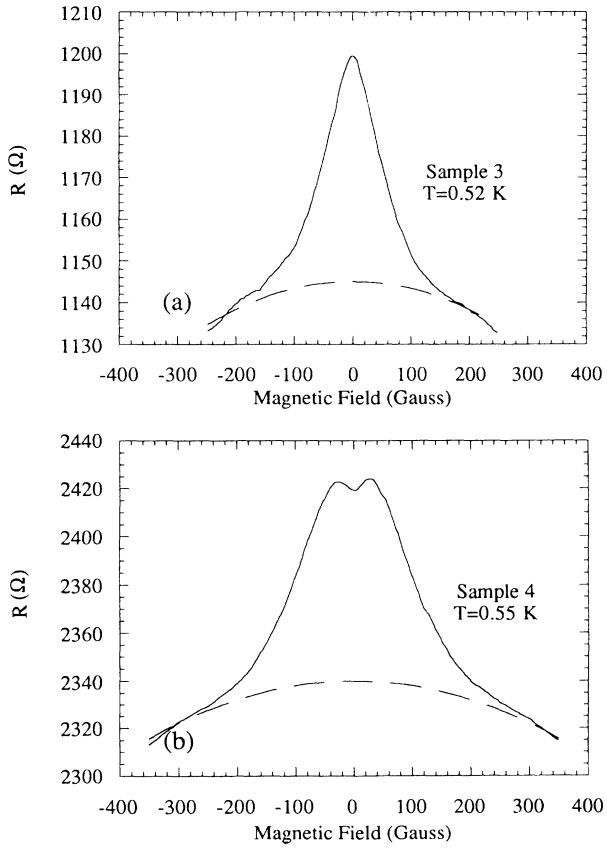

FIG. 2. Low-field magnetoresistance of the narrow wires of the (a) GaAs/AlGaAs and (b) pseudomorphic $Ga_xIn_{1-x}As/Al_xIn_{1-x}As$ samples in a perpendicular magnetic field. Dashed lines are the temperature-independent parabolic background resistances.

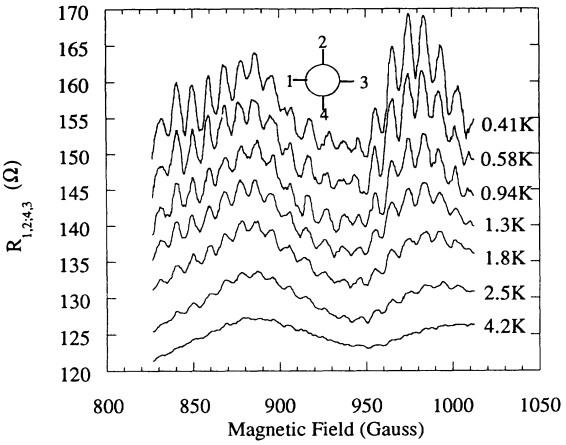

FIG. 3. The four-point resistance $R_{1,2;3,4}$ vs magnetic field at different temperatures for the 7.8-μm perimeter ring of sample 1 ($GaAs/Al_xGa_{1-x}As$). The leads 1, 2, 3, and 4 are shown at the upper side of the figure. The y axis is given for the 4.2 K data; all the others are displaced by 10Ω from each other.

material. The data of different temperatures are very correlated, and the peak positions in a magnetic field do not move even though the sizes of the oscillations are attenuated with increasing temperature. The background resistance is due to universal conductance fluctuations and is easily separable from the AB oscillations in the Fourier spectra even at the highest temperature.

In order to get a better temperature range for each ring, we focused our four-point resistance measurements in a magnetic-field range which showed the largest AB oscillations. Typically, the chosen magnetic-field range would include 15 to 20 periods of AB oscillations. An unnormalized root mean square of AB conductances

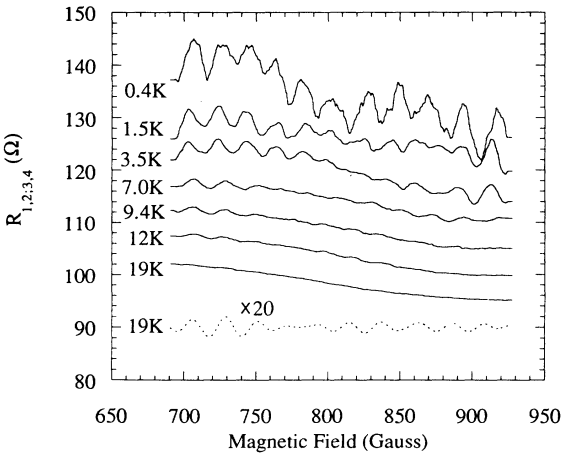

FIG. 4. Same as Fig. 3 for the 5.2-μm perimeter ring of sample 2 (pseudomorphic $Ga_xIn_{1-x}As/Al_xIn_{1-x}As$). The y axis is given for the 19 K data; the others are displaced by 5Ω from each other. AB oscillations are resolved up to 19 K in this sample. The dashed line shows the 19-K data after the background resistance is subtracted.

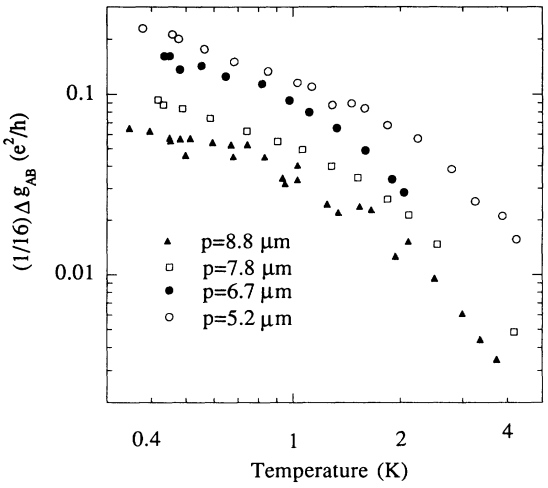

FIG. 5. Root-mean-square AB magnetoconductance Δg_{AB} vs temperature for all four rings of $GaAs/Al_xGa_{1-x}As$ sample.

$\tilde{\Delta}g_{AB}$ is obtained from this limited magnetic-field range. To normalize $\tilde{\Delta}g_{AB}$, first magnetoresistance data are taken in a much wider magnetic-field range at 0.4 K. Next $\tilde{\Delta}g_{AB}$ is scaled by a number such that Δg_{AB} at 0.4 K would be the same as the rms AB conductance of the wider magnetic-field range. Figure 5 shows the rms AB conductances Δg_{AB} which are scaled in this manner versus temperature for all four rings of the $GaAs/Al_xGa_{1-x}As$ sample. As expected from the exponential term $\exp(-\alpha p/l_\phi)$ in the AB scaling equation, the amplitudes of the AB oscillations are smaller for bigger perimeter rings and get smaller with increasing temperature due to the decrease in l_ϕ.

Our ring geometry, schematically shown in Fig. 1(b), has the advantage of having a higher relative amplitude of AB oscillations in conductance, $\Delta g_{AB}=\Delta R_{AB}/R^2$, in comparison to the commonly used double connected ring geometry of Fig. 1(a).[25] The background resistance R of our geometry is expected to be four times smaller than the background resistance of the doubly connected ring geometry, therefore in order to compare our results with similar experiments, we further scaled in Fig. 5 our AB amplitudes in conductance, $\Delta g_{AB}=\Delta R_{AB}/R^2$, by a factor of $\frac{1}{16}$. Here we assumed that ΔR_{AB}'s are not very different for different geometries, which is experimentally supported by the observed correlations in the four-point AB resistance oscillations.[26]

IV. DATA ANALYSIS

Typically, in quasi-one-dimensional wires the material parameters can be quite different than the two-dimensional ones due to boundary scattering effects and reduced dimensionality.[27] In the absence of spin-orbit scattering the weak-localization formula [Eq. (5)] contains three parameters: τ_ϕ, τ_e, and w. In the presence of spin-orbit scattering Eq. (10) contains the additional parameter τ_{SO}. For a given sample τ_ϕ and in principle τ_{SO} are temperature dependent whereas τ_e and w remain con-

stant for the entire temperature study range. Similar to other groups,[6–10] by using the equation for background conductance $G_{cl}=me^2Dw/\pi\hbar^2L$ where $D=v_f^2\tau_e/2$ and the measured G_{cl}, we reduce the number of unknown parameters by eliminating either w or τ_e. Due to sidewall depletion the electrical width of the wires can be significantly smaller than the pattern width which was 0.45 μm in our wires. In some samples, independent information about the electrical width of the wires can be obtained from Shubnikov–de Haas oscillations.[28] In two dimensions, a plot of the filling factor n versus the reciprocal of the SdH peak position in magnetic field would give a straight line. Figure 6 shows such a plot for the narrow wires of sample 4. There is a deviation from the straight-line behavior (shown by the solid line) at low magnetic fields where the width of the wire is comparable to the cyclotron radius. The data can be fitted by the analytic expression given by Berggren *et al.* which assumes a parabolic confinement potential. From this fit we obtain the width of the wires of sample 4 as 0.21 μm. Thus, knowing the carrier density and the width of the wires, we get D and τ_e directly from the background conductance G_{cl} of this sample. However, in similar plots of SdH peak positions for the narrow wires of the other samples, we could not resolve significant deviations from the straight-line behavior. Therefore, we had to take τ_e or w as an extra parameter in the analysis of the weak-localization data of these samples.

The phase-coherence length l_ϕ (or τ_ϕ), which is the key material parameter in all quantum interference effects, has always been taken as an adjustable parameter. We aimed to demonstrate consistency of the l_ϕ's obtained from the weak-localization and AB effects.

We will first present the analysis of the data obtained from the $GaAs/Al_xGa_{1-x}As$ samples which did not show significant spin-orbit interaction. Then, we will continue with the data of the pseudomorphic $Ga_xIn_{1-x}As/Al_xIn_{1-x}As$ samples, and focus on the modifications in quantum interference effects due to spin-orbit interaction. Last, we will compare the l_ϕ's obtained from our data with the theoretically expected ones.

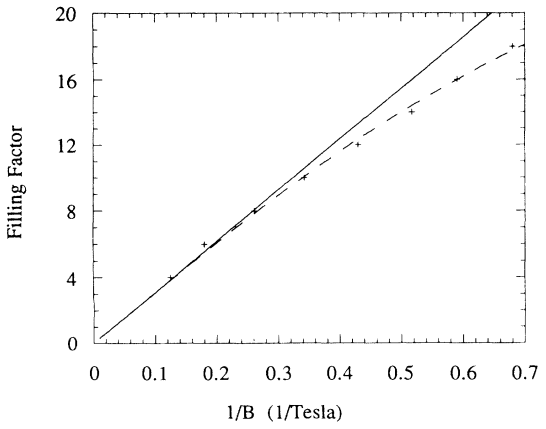

FIG. 6. Filling factor n vs the reciprocal of the SdH peak position obtained from the four-point magnetoresistance of the narrow wires of sample 4 (pseudomorphic $Ga_xIn_{1-x}As/Al_xIn_{1-x}As$). The solid line represents the expected behavior in two-dimensional systems. The dashed line is the theoretical fit which assumes a parabolic confinement potential. The fit gives a width of 0.21 μm and a carrier density of 0.8×10^{12} cm^{-2}.

A. $GaAs/Al_xGa_{1-x}As$ samples

1. *Weak localization*

Low-field magnetoconductance data of the WL sample fabricated on the $GaAs/Al_xGa_{1-x}As$ heterostructure can be analyzed by both AA [Eqs. (2) and (2)] and BvH [Eqs. (4) and (5)] theories which do not include spin-orbit coupling. We assumed that the boundary scatterings were specular,[6] and therefore used $K_1=0.11$ and $K_2=0.23$. Even though our wires were ballistic, by taking τ_ϕ and τ_e as our fitting parameters and by only allowing τ_ϕ to change as a function of temperature, both theories fit the experiment successfully (Fig. 7). However, the main fitting parameters τ_ϕ obtained from the two theories were quite different in magnitude. For instance, we obtained a τ_ϕ of 51 and 10 psec from the BvH and AA fits of the magnetoconductance data at 0.41 K, respectively. The AA theory gave an l_e of 3.2 μm, much bigger than the width of the wires which violates the applicability of this theory. So, even though both of the theories fit the experiment equally well, the BvH theory appears to be physically more meaningful.

2. *Ab effect*

We also studied the AB effect in this material on four different-sized rings. The phase-coherence length $l_\phi(T)$ can be obtained just from the amplitude of the AB oscillations by using either Eqs. (6) or (7), if the numerical prefactor γ is known. Since different rings have the same geometry, we assume that the prefactor γ and the phase-coherence length $l_\phi(T)$ in the scaling equations (6) and (7)

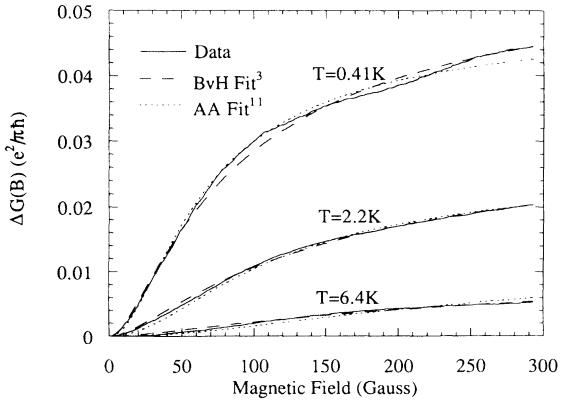

FIG. 7. Low-field magnetoconductance $\Delta G(B)$ of the narrow wires of the $GaAs/Al_xGa_{1-x}As$ sample in units of $e^2/\pi\hbar$ at different temperatures. The data is fitted using BvH (Ref. 3) [Eqs. (4) and (5)] and AA (Ref. 11) [Eqs. (2) and (3)] theories. The fitting parameters are τ_ϕ and τ_e.

are the same for the different-sized rings of the same sample. At each temperature, we estimate γ by fitting Δ_{gAB} versus p using the scaling equations. We performed this fitting by using both of the scaling equations at eight different temperatures to obtain an average of γ's, and used this γ_{av} to obtain $l_\phi(T)$. As expected from the theory, γ_{av} obtained from either Eqs. (6) or (7) (1.2 and 0.9, respectively) were on the order of unity. Figure 8 shows the phase-coherence lengths extracted in this manner. In the temperature range of our experiment, $l_{\phi AB}$ (1.5–4 μm) was smaller than the perimeters of the rings, so the exponential terms in the AB scaling equations were dominant. The error bars are obtained from the deviation in γ, and they get smaller at higher temperatures, since the exponential term of the scaling equation becomes more dominant, and therefore the error in γ becomes less important. Since the difference between Eqs. (6) and (7) is only in the prefactors, the phase-coherence lengths obtained using these equations did not differ much from each other, and both are in close agreement to within 15% with the independently extracted phase-coherence lengths from weak-localization data using BvH theory. This observation indicates that these two different quantum interference effects are governed by the same l_ϕ. On the other hand, the AA theory gives values which are substantially smaller for l_ϕ which strongly suggests, as we anticipated earlier, that this theory is not applicable to our wires. We conclude that the BvH theory gives the right physics in ballistic wires and indeed flux cancellation mechanisms are in effect.

As shown in Fig. 8, in the temperature range of the experiment, the thermal length L_T is much smaller than the perimeters of the AB rings, which was the necessary condition for using energy averaging prefactors in scaling Eqs. (6) and (7).

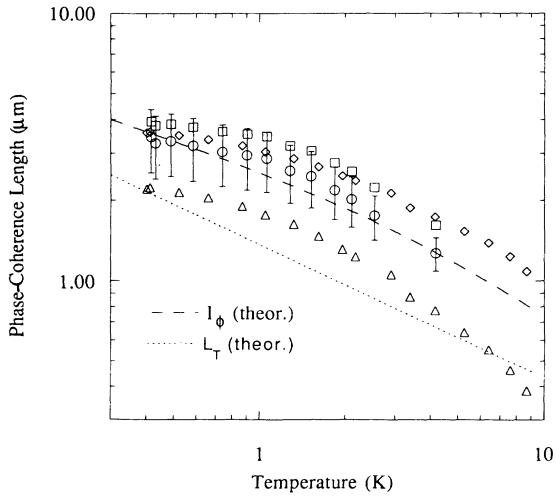

FIG. 8. Phase-coherence lengths obtained from the weak-localization (using BvH ◇ and AA △ theories) and AB data [using Eq. (6) (□) and (7) (○)] vs temperature for the narrow wires fabricated on the GaAs/$Al_xGa_{1-x}As$ heterostructure. Theoretical l_ϕ and thermal length L_T are also shown in the figure.

B. Pseudomorphic $Ga_xIn_{1-x}As/Al_xIn_{1-x}As$ samples

1. *Weak localization*

Four-point magnetoresistance data of the pseudomorphic $Ga_xIn_{1-x}As/Al_xIn_{1-x}As$ narrow wire samples are fitted using the one-dimensional weak-localization theory modified to include spin-orbit interaction [Eq. (10)]. Again, we assumed specular boundary scatterings. For sample 4, since the width of the wires was known from SdH peak positions (Fig. 6), we had only two fitting parameters, τ_ϕ and τ_{SO}; furthermore we did not allow τ_{SO} to change as a function of temperature. As shown in Fig. 9(a), the agreement between the experiment and theory is much better when the BvH theory [Eq. (4)] is used, especially at the lowest temperature where the AA theory failed to give the right magnetic-field scale. This is direct evidence that the flux cancellation mecha-

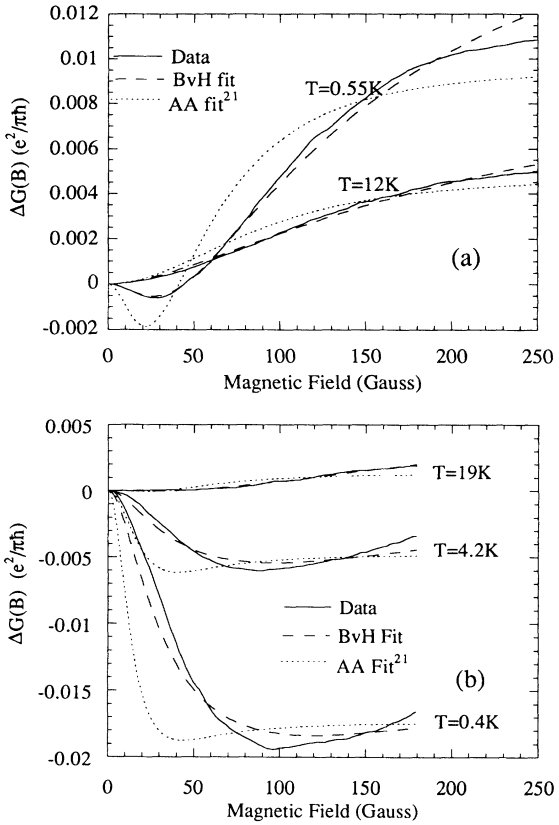

FIG. 9. Low-field magnetoconductance $\Delta G(B)$ of the narrow wires of the pseudomorphic $Ga_xIn_{1-x}As/Al_xIn_{1-x}As$ samples after the parabolic background resistance is subtracted in units of $e^2/\pi\hbar$ ar different temperatures. The data is fitted using the modified BvH and AA theories which take into account spin-orbit interactions (Ref. 21). The fits for sample 4 are shown in (a) where the fitting parameters are τ_ϕ and τ_{SO} (for $T=0.55$ K data: $\tau_\phi=50$ psec, $\tau_{SO}=46$ psec from the BvH fit; $\tau_\phi=32$ psec, $\tau_{SO}=26$ psec from the AA fit). The fits for sample 5 are shown in (b) where the fitting parameters are τ_ϕ, τ_{SO}, and τ_e (for $T=0.4$ K data: $\tau_\phi=48$ psec, $\tau_{SO}=13$ psec, and $\tau_e=2.4$ psec from the BvH fit; $\tau_\phi=20$ psec, $\tau_{SO}=3$ psec, and $\tau_e=2.5$ psec from the AA fit).

TABLE II. Elastic and spin-orbit scattering times obtained from BvH fits, widths of the wires, diffusion constants, and zero-magnetic-field background resistances for all weak-localization samples.

	τ_e (psec)	τ_{SO} (psec)	w (μm)	D (m^2/sec)	R_{bg} ($k\Omega$)
Sample 3	5.1		0.24	0.24	1.1
Sample 4	1.3	46	0.21	0.18	2.3
Sample 5	2.4	13	0.26	0.65	0.52

nism occurs in our narrow wires. We got $\tau_{SO}=46$ psec and a range of τ_ϕ's from 8 to 54 psec from the BvH fit of the weak-localization data of this sample. Similarly, for sample 5 the magnetoresistance data are only fitted reasonably [Fig. 9(b)] with the modified one-dimensional BvH theory which includes spin-orbit interaction and the flux cancellation mechanism. In this sample, spin-orbit interaction ($\tau_{SO}=13$ psec) was even stronger due to higher carrier concentration. This sample is also more ballistic (higher l_e/w) compared to sample 4, therefore the conductance minima occurred at a higher magnetic field. Unlike two-dimensional systems, in one-dimensional ballistic wires the magnetic-field position of the conductance minima is not just determined by l_{SO}. We roughly estimated this position, using $\tau_B=\tau_{SO}$, as 50 and 100 G for samples 4 and 5, respectively.

Elastic and spin-orbit scattering times obtained from BvH fits, widths of the wires, diffusion constants, and zero-magnetic-field background resistances for all weak-localization samples are summarized in Table II.

2. *AB effect*

It is difficult to extract phase-coherence length from the amplitude of the AB oscillations of the pseudomorphic $Ga_xIn_{1-x}As/Al_xIn_{1-x}As$ sample due to the strong spin-orbit interaction in this material: first, there is a new unknown parameter, spin-orbit scattering length l_{SO} involved in the scaling theory of AB oscillations, and second, the analytical form of the amplitude of the AB oscillations in the presence of spin-orbit scattering is not known. Therefore, instead of trying to extract l_ϕ from the AB data of this sample we fitted the amplitudes of the AB oscillations with the different AB scaling equations discussed earlier. This way we can compare our data with the AB theories which do and do not take into account spin-orbit scatterings.

The amplitudes of the AB oscillations Δg_{AB} of different-perimeter rings are fitted by taking γ as an adjustable parameter and using the phase-coherence lengths and the spin-orbit scattering length obtained from the weak-localization fitting of the magnetoconductance of the narrow wires of sample 5 which has the same carrier density as the AB sample. The fits by using different scaling equations for the 5.2 and 7.8-μm perimeter rings of this sample are shown in Fig. 10.

As mentioned before, the energy averaging prefactor used in Eq. (6) is not quite correct. For this equation, spin-orbit reduction factors are temperature independent, and therefore, the scaling equation does not change with the introduction of spin-orbit interaction. Equation (7), which we believe has a more realistic energy averaging prefactor, did not agree with the experimentally measured amplitudes of the AB magnetoresistance oscillations. However, by the introduction of spin-orbit reduction factors to Eq. (7) [Eq. (13)], we get the best agreement with the experiment. Even though we could not exactly fit the amplitudes of the AB oscillations, the significant improvement of the fit from Eq. (7) to Eq. (13) is an evidence for the presence of spin-orbit interaction related reductions in the amplitude of the AB oscillations. A more realistic scaling equation is necessary to have a better analysis of the size of the AB oscillations of this experiment.

C. Phase-coherence length

The main dimensional scales in quantum interference effects are set by phase relaxation mechanisms. At low temperatures, it is believe that electron-electron interactions are the dominant mechanism for the phase relaxation of electrons. In one-dimensional wires, when $w<\pi L_T$, phase-coherence time is given by

$$\frac{1}{\tau_\phi}=\frac{\pi}{2}\frac{(kT)^2}{\hbar E_f}\ln\frac{E_f}{kT}+\left[\frac{\pi kT}{D^{1/2}wm^*}\right]^{2/3}. \tag{14}$$

The first term in this equation is due to momentum conserving processes[29] and becomes dominant at relatively higher temperatures, whereas the second term, also

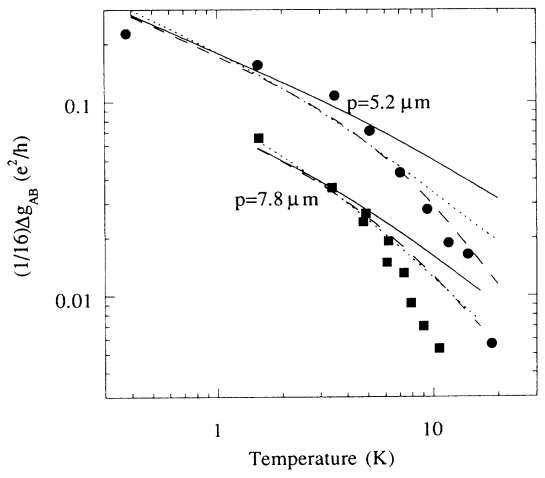

FIG. 10. Root-mean-square AB magnetoconductance Δ_{gAB} vs temperature for the rings with perimeters of 5.2 and 7.8 μm of sample 2. The data is fitted using Eqs. (6), (7), and (13) which are shown by dotted, solid, and dashed lines, respectively. In equation (13) $E_c=(\hbar D/p^{0.7}l_\phi^{1.3})$ is used and γ is taken as an adjustable parameter.

known as Nyquist time, is due to momentum nonconserving processes[30] which leads to a $T^{-1/3}$ behavior of l_ϕ at very low temperatures. The Nyquist time has been observed in various one-dimensional systems.[31,32] However, two groups recently measured, one using weak localization[7] and the other using universal conductance fluctuations,[1] a temperature-independent l_ϕ at low temperatures in quasi-one-dimensional wires fabricated on $GaAs/Al_xGa_{1-x}As$ heterostructure.

For our wires, we calculated the theoretical l_ϕ (T) using Eq. (14) and the material parameters obtained from BvH fitting of the weak-localization data. In the $GaAs/Al_xGa_{1-x}As$ heterostructure, theoretical l_ϕ is in good agreement with the experimental l_ϕ's either from the amplitude of the AB oscillations or from weak-localization data when the BvH theory is used (Fig. 8). On the other hand, in the pseudomorphic $Ga_xIn_{1-x}As/Al_xIn_{1-x}As$ heterostructure experimental l_ϕ's, especially at high temperatures, were about a factor 2 higher than the theoretically predicted ones [Figs. 11(a) and 11(b)]. Since no adjustable parameters were used in the calculation of l_ϕ, the order-of-magnitude agreement between the experimental and theoretical l_ϕ's is acceptable. However, the increase in measured l_ϕ's as temperature goes to zero was slower than the theoretically expected $T^{-1/3}$ dependence. The origin of such deviations has not yet been understood.

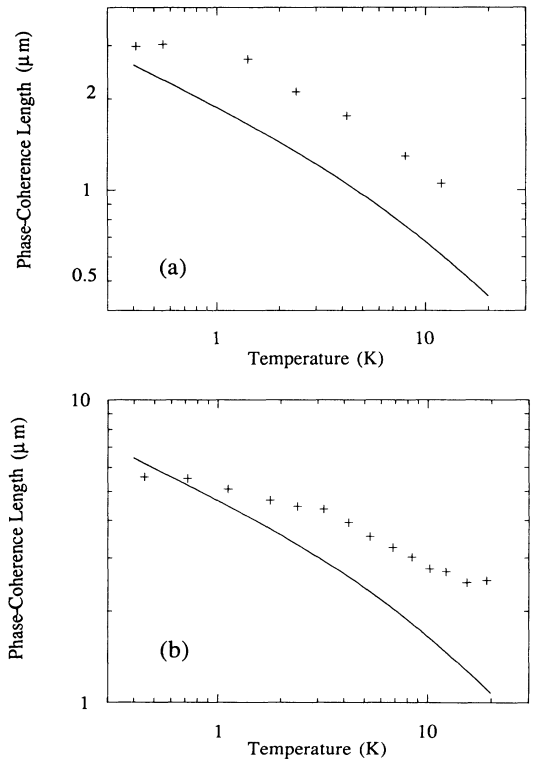

FIG. 11. Phase-coherence lengths obtained from the weak-localization fitting [Eqs. (4) and (10)] of the magnetoconductance data of the pseudomorphic $Ga_xIn_{1-x}As/Al_xIn_{1-x}As$ samples vs temperature [sample 4 in (a) and sample 5 in (b)]. Solid lines show the theoretical l_ϕ's.

V. CONCLUSIONS

In summary, we studied quantum interference effects in very narrow wires where the width is much smaller than the elastic-scattering length. We verified directly that flux cancellation mechanisms are present in these quasi-one-dimensional wires. The weak-localization data were in good agreement with the theories that included flux cancellation mechanisms.

The systematic study of the Aharonov-Bohm effect in different-sized rings fabricated on the $GaAs/Al_xGa_{1-x}As$ heterostructure which did not show significant spin-orbit coupling made it possible to extract useful information, phase-coherence length, from the size of the AB magnetoresistance oscillations. Phase-coherence lengths obtained from the AB magnetoresistance oscillations were in close agreement with the l_ϕ independently obtained from weak localization.

The pseudomorphic $Ga_xIn_{1-x}As/Al_xIn_{1-x}As$ heterostructure showed strong spin-orbit interaction which modifies quantum interference effects significantly. Experimentally, the influence of spin-orbit coupling on weak localization is identified easily, since there is a change in the sign of magnetoresistance. We modified the BvH theory of weak localization by including spin-orbit scatterings which fitted the magnetoresistance data of our narrow wires which are fabricated on the pseudomorphic $Ga_xIn_{1-x}As/Al_xIn_{1-x}As$ heterostructure. On the other hand, the influence of spin-orbit coupling on the Aharonov-Bohm effect is more difficult to observe, since in the strong spin-orbit-scattering limit the correction factor is $\frac{1}{2}$ and it is inevitably mixed with the sample-dependent prefactor γ. Our asymptotic analysis of the AB scaling equation in the strong spin-orbit-scattering regime suggests reduction factors for the amplitude of the AB oscillations which gets smaller with increasing temperature. With the introduction of the spin-orbit reduction factors, there was less discrepancy between the measured amplitudes of the AB oscillations and the expected amplitudes obtained by using the phase-coherence lengths extracted from weak-localization data. This is the first observation of the influence of spin-orbit interaction on the AB effect.

Phase relaxation mechanisms in quasi-one-dimensional wires are not well understood. Similar to few other groups, we observed deviations in l_ϕ from the theoretically expected $T^{-1/3}$ behavior at low T, however saturation has not been observed down to $T=0.35$ K. Further work needs to be done at lower temperatures $T<0.35$ K to elucidate the mechanism for phase relaxation in semiconductor narrow wires.

ACKNOWLEDGMENTS

We would like to thank Professor D. C. Tsui for many useful discussions and one of us (Ç.K.) would like to thank him for his encouragement throughout this work. Ç. Kurdak is partially supported by NSF Grant No. DMR-90-16024 at Princeton University.

[1]J. P. Bird, A. D. C. Grassie, M. Lakrimi, K. M. Hutchings, A. P. Meeson, J. J. Harris, and C. T. Foxon, J. Phys. Condens. Matter **3**, 2897 (1991).
[2]V. K. Dugaev and D. E. Khemel'nitskii, Zh. Eskp. Teor. Fiz. **86**, 1784 (1984) [Sov. Phys. JETP **59**, 1038 (1984)].
[3]C. W. Beenakker and H. van Houten, Phys. Rev. B **38**, 3232 (1988).
[4]R. J. Elliot, Phys. Rev. **96**, 266 (1954).
[5]O. Millo, S. J. Klepper, M. W. Keller, D. E. Prober, S. Xiong, and A. D. Stone, Phys. Rev. Lett. **65**, 1494 (1990).
[6]H. van Houten, C. W. Beenakker, B. J. van Wees, and J. E. Mooij, Surf. Sci. **196**, 144 (1988).
[7]T. Hiramoto, K. Hirakawa, Y. Iye, and T. Ikoma, Appl. Phys. Lett. **54**, 2103 (1989).
[8]Y. Takagaki, K. Ishibashi, S. Ishida, S. Takaoka, K. Gamo, K. Murase, and S. Namba, Jpn. J. Appl. Phys. **28**, 645 (1989).
[9]S. K. Greene, M. Pepper, D. C. Peacock, D. A. Ritchie, V. J. Law, R. Newbury, J. E. F. Frost, R. J. Brown, H. Ahmed, and D. Hasko (unpublished).
[10]A. M. Chang, G. Timp, T. Y. Chang, J. E. Cunningham, B. Chelluri, P. Mankiwich, R. Behringer, and R. E. Howard, Surf. Sci. **196**, 46 (1988).
[11]B. L. Al'tshuler and A. G. Aronov, Pis'ma Zh. Eksp. Teor. Fiz. **33**, 515 (1981) [JETP Lett. **33**, 499 (1981)].
[12]S. Hikami, A. I. Larkin, and Y. Nagaoka, Prog. Theor. Phys. **63**, 707 (1980).
[13]G. Bergman, Phys. Rev. Lett. **48**, 1046 (1982).
[14]Y. Kawaguchi, I. Takayanagi, and S. Kawaji, J. Phys. Soc. Jpn. **56**, 1293 (1987).
[15]Y. Meir, Y. Gefen, and O. Etin-Wohlmon, Phys. Rev. Lett. **63**, 798 (1989).
[16]S. Chakravarty and A. Schmid, Phys. Rep. **140**, 193 (1986).
[17]P. A. Lee and A. D. Stone, Phys. Rev. Lett. **55**, 1622 (1985).
[18]S. Washburn, C. P. Umbach, R. B. Laibowitz, and R. A. Webb, Phys. Rev. B **32**, 4789 (1985).
[19]F. P. Milliken, S. Washburn, C. P. Umbach, R. B. Laibowitz, and R. A. Webb, Phys. Rev. B **36**, 4465 (1987).
[20]D. P. DiVincenzo and C. L. Kane, Phys. Rev. B **38**, 3006 (1988).
[21]P. Santhanam, S. Wind, and D. E. Prober, Phys Rev. Lett. **53**, 1179 (1984).
[22]A. Chin and T. Y. Chang, J. Vac. Sci. Technol. B **8**, 364 (1990).
[23]K. Owusu-Sekyere, A. M. Chang, and T. Y. Chang, Appl. Phys. Lett. **52**, 1246 (1988).
[24]K. K. Choi, D. C. Tsui, and S. C. Palmateer, Phys. Rev. B **33**, 8216 (1986).
[25]G. Timp, A. M. Chang, T. Y. Chang, J. E. Cunningham, P. Mankiewich, R. Behringer, and R. E. Howard, Phys. Rev. Lett. **58**, 2814 (1987); C. J. B. Ford, T. J. Thrornton, R. Newbury, M. Pepper, H. Ahmed, D. C. Peacock, D. A. Ritchie, J. E. F. Frost, and G. A. C. Jones, Appl. Phys. Lett. **54**, 21 (1989).
[26]A. M. Chang, K. Owusu-Sekyere, and T. Y. Chang, Solid State Commun. **67**, 1027 (1988).
[27]H. Z. Zheng, H. P. Wei, D. C. Tsui, and G. Weimann, Phys. Rev. B **34**, 5635 (1986).
[28]K.-F. Berggren, G. Roos, and H. van Houten, Phys. Rev. B **37**, 10 118 (1988); J. F. Weisz and K.-F. Berggren, *ibid.* **40**, 1325 (1989).
[29]H. Fukiyama and E. Abrahams, Phys. Rev. B **27**, 5976 (1983).
[30]B. L. Al'tshuler, A. G. Aronov, and D. E. Khemel'nitskii, J. Phys. C **15**, 7367 (1982); Solid State Commun. **39**, 619 (1981).
[31]J. J. Lin and N. Giordano, Phys. Rev. B **33**, 1519 (1986).
[32]K. K. Choi, D. C. Tsui, and K. Alavi, Phys. Rev. B **36**, 7751 (1987).